

This is an Open Access document downloaded from ORCA, Cardiff University's institutional repository:<https://orca.cardiff.ac.uk/id/eprint/123086/>

This is the author's version of a work that was submitted to / accepted for publication.

Citation for final published version:

Munir, Arooj, Døskeland, Anne, Avery, Steven J., Fuoco, Tiziana, Mohamed-Ahmed, Samih, Lygre, Henning, Finne-Wistrand, Anna, Sloan, Alastair J. , Waddington, Rachel J. , Mustafa, Kamal and Suliman, Salwa 2019. Efficacy of copolymer scaffolds delivering human demineralised dentine matrix for bone regeneration. *Journal of Tissue Engineering* 10 , p. 204173141985270. 10.1177/2041731419852703

Publishers page: <http://dx.doi.org/10.1177/2041731419852703>

Please note:

Changes made as a result of publishing processes such as copy-editing, formatting and page numbers may not be reflected in this version. For the definitive version of this publication, please refer to the published source. You are advised to consult the publisher's version if you wish to cite this paper.

This version is being made available in accordance with publisher policies. See <http://orca.cf.ac.uk/policies.html> for usage policies. Copyright and moral rights for publications made available in ORCA are retained by the copyright holders.



Efficacy of copolymer scaffolds delivering human demineralised dentine matrix for bone regeneration

Journal of Tissue Engineering
Volume 10: 1–16
© The Author(s) 2019
Article reuse guidelines:
sagepub.com/journals-permissions
DOI: 10.1177/2041731419852703
journals.sagepub.com/home/tej



Arooj Munir¹, Anne Døskeland², Steven J Avery^{3,4},
Tiziana Fuoco⁵, Samih Mohamed-Ahmed¹, Henning Lygre¹,
Anna Finne-Wistrand⁵, Alastair J Sloan^{3,4} , Rachel J Waddington^{3,4},
Kamal Mustafa¹ and Salwa Suliman¹ 

Abstract

Poly(L-lactide-co- ϵ -caprolactone) scaffolds were functionalised by 10 or 20 $\mu\text{g}/\text{mL}$ of human demineralised dentine matrix. Release kinetics up to 21 days and their osteogenic potential on human bone marrow stromal cells after 7 and 21 days were studied. A total of 390 proteins were identified by mass spectrometry. Bone regeneration proteins showed initial burst of release. Human bone marrow stromal cells were cultured on scaffolds physisorbed with 20 $\mu\text{g}/\text{mL}$ and cultured in basal medium (DDM group) or physisorbed and cultured in osteogenic medium or cultured on non-functionalised scaffolds in osteogenic medium. The human bone marrow stromal cells proliferated less in demineralised dentine matrix group and activated ERK1/2 after both time points. Cells on DDM group showed highest expression of IL-6 and IL-8 at 7 days and expressed higher collagen type I alpha 2, SPPI and bone morphogenetic protein-2 until 21 days. Extracellular protein revealed higher collagen type I and bone morphogenetic protein-2 at 21 days in demineralised dentine matrix group. Cells on DDM group showed signs of mineralisation. The functionalised scaffolds were able to stimulate osteogenic differentiation of human bone marrow stromal cells.

Keywords

Growth factor, mesenchymal stem cell, bone tissue engineering, drug delivery, functionalisation

Date received: 4 March 2019; accepted: 3 May 2019

Introduction

Despite the fact that different treatment modalities are available for bone defect healing, critical-sized defects still pose a clinical challenge.¹ To overcome the limitations of current treatment modalities, alternative potent bone substitutes or osteoinductive three-dimensional (3D) scaffolds are required for restoring the function and structure of tissue, not only by osteoconduction but also to deliver growth factors/bioactive molecules to instruct the body's own mechanism for regeneration.² Natural bone healing is a complex process and occurs in the presence of a cocktail of growth factors working synergistically to modulate signal transduction, cell proliferation, migration and differentiation.³

¹Centre for Clinical Dental Research, Department of Clinical Dentistry, Faculty of Medicine, University of Bergen, Bergen, Norway

²Department of Biomedicine, University of Bergen, Bergen, Norway

³Department of Oral and Biomedical Sciences, School of Dentistry, Cardiff University, Cardiff, UK

⁴Cardiff Institute for Tissue Engineering and Repair (CITER), Cardiff, UK

⁵Department of Fibre and Polymer Technology, KTH Royal Institute of Technology, Stockholm, Sweden

Corresponding authors:

Salwa Suliman, Centre for Clinical Dental Research, Department of Clinical Dentistry, Faculty of Medicine, University of Bergen, 5009 Bergen, Norway.

Email: salwa.suliman@uib.no

Kamal Mustafa, Department of Clinical Dentistry, Faculty of Medicine, University of Bergen, 5009 Bergen, Norway.

Email: kamal.mustafa@uib.no



The tooth, comprised of enamel, dentine, pulp and cementum, is the hardest structure in the body after bone.⁴ Dentine forms the bulk of the tooth matrix and has a chemical composition by weight/volume made up of approximately 70% mineral (hydroxyapatite), 18% organic (collagen), 2% inorganic (non-collagenous proteins) and 10% body fluid.⁴ Dentine not only provides structural support but it is also a source of bioactive growth factors;⁵ the necessity of growth factors acting synergistically for regeneration is well reported.⁶ Bone formation by human demineralised dentine matrix (hDDM) is a complex process and is not completely understood. It is believed that the signal transduction by the presence of bioactive molecules is the key element for initiating regeneration.^{7–9} The major collagen in hDDM is type 1, which provides a matrix necessary for hydroxyapatite mineral deposition. Non-collagenous proteins include decorin, biglycan, dentine sialophosphoprotein, dentine phosphoprotein, bone sialoprotein, osteopontin, osteoglycin, osteomodulin, extracellular matrix (ECM) and fibromodulin. These proteins regulate mineral deposition, cell signalling, differentiation and survival.^{7,8,10,11} Proteomic analyses on dentine have identified 147–289 proteins,^{5,8} and enzyme-linked immunosorbent assay (ELISA) in our recent study showed the presence of transforming growth factor beta 1 (TGF- β 1), bone morphogenetic proteins (BMPs), fibroblast growth factor (FGF) and vascular endothelial growth factor (VEGF).⁹ In dentine, presence of soluble collagens, non-collagenous proteins¹⁰ and growth factors stimulates the cellular responses, and hence are responsible for dentine's ability to regenerate.⁸ It has been reported that DDM obtained from demineralisation of dentine has shown a high potential for mesenchymal stem cells (MSCs) to migrate, proliferate and differentiate,⁹ as well as promote bone formation in calvaria bone defects in rats¹² and blood vessel formation in tooth socket of rats.¹³ Lee et al.⁷ reported that dental pulp stem/progenitor cells (DPSC) showed improved wound healing and mineralisation in response to hDDM. Interestingly, in vivo, the bone formed by hDDM was histologically comparable to the bone formed using autogenous bone grafts.¹⁴ Thus, the natural regenerative property of hDDM caused it to gain attention as an alternative for conventional bone substitutes in bone tissue engineering.¹⁵

Clinically, hDDM has been used successfully as a graft for socket preservation,¹⁶ implant stability and guided bone regeneration,¹⁷ sinus lift and ridge augmentation¹⁸ as a bolus to the bony defects, either as powder or block or as a carrier for recombinant BMP-2. The mode of delivering growth factors to a bone defect is an important factor to optimise their biological function and efficacy,¹⁹ and studies reported supra-physiological doses to have harmful effects.²⁰ To date, DDM has been delivered as a supplement in cell culture medium (in vitro), replaced continuously with every medium change and as a powder or tissue block (in vivo), thus delivering growth factors in a bulk

supply. These methods can cause a burst release of the growth factors, which are eventually washed away, with no spatiotemporal control. The direct application of hDDM on cells in vitro presented with different responses, namely, hDDM at low concentrations (0.1 μ g/mL), acts as a chemo-attractant for cells, in contrast to higher concentrations (10 μ g/mL), where it promotes cell differentiation.⁷ Our recent report showed that incorporation of 10 μ g/mL hDDM in liposomes for the regeneration of dental tissue enhanced DPSC migration compared to when free hDDM was used, due to the controlled release of a cocktail of growth factors from hDDM.²¹ Therefore, a suitable physiological delivery method such as a 3D scaffold is necessary for a controlled delivery of hDDM in a spatiotemporal manner while simultaneously providing provisional structural support in the bone defect.

The degradable aliphatic polyester, copolymer of L-lactide and ϵ -caprolactone (poly(LLA-co-CL)) have been comprehensively studied by our group and proven to be a cyto-compatible and osteoconductive scaffold for bone tissue engineering.²² It has been rendered osteoinductive by functionalising to deliver the most studied growth factor in bone regeneration, BMP-2.^{19,23}

In this study, poly(LLA-co-CL) scaffolds were physisorbed with hDDM to deliver a cocktail of growth factors similar to the bone healing cascade of events and simultaneously provide 3D provisional support to the bone defect.

Materials and methods

Poly(LLA-co-CL) scaffold fabrication

Poly(LLA-co-CL) scaffolds were prepared by the solvent-casting particulate leaching method described previously.²⁴ Copolymer ('Resomer LC 703 S', Evonik, Essen, Germany), with molecular weight $M_n = 142 \text{ kg mol}^{-1}$ ($\bar{D} = 1.5$) and composition in mole ratio of 70 for L-lactide = 70 and 30 for ϵ -caprolactone, was dissolved in chloroform (0.1 g/mL). The polymer solution was added into a mould containing sodium chloride particles with a ratio of polymer to salt as 1:10. Following the evaporation of chloroform, scaffolds were punched out in sizes of 12 mm diameter and 1.3 mm thickness and salt particles were leached by continuous soaking for 3 days in deionised water. Scaffolds were washed with ethanol and sterilised under ultraviolet light. The scaffold porosity was >83%, and it had a pore size of 90–500 μ m, measured by micro computed tomography (Skyscan 1172, Bruker, MA, US) (40 kV and 2.4 micron voxel).

Preparation of hDDM

The hDDM was prepared as described previously.⁷ Briefly, healthy human teeth were obtained from Cardiff University School of Dentistry Tissue bank with informed patient consent in accordance with ethical approval granted by South

East Wales Research Ethics Committee (12/WA/0289). Pulp, gingiva enamel and cementum were removed, and the remaining dentine was powdered using a ball and mill in liquid nitrogen. Dentine matrix was suspended in 7.5% ethylenediaminetetraacetic acid (EDTA) (pH 7.2), containing protease inhibitor, 1 mM iodoacetic acid, 5 mM n-ethylmaleimide and 5 mM benzamide HCl at 4°C for 2 weeks. EDTA supernatant, containing extracted non-collagenous proteins and soluble collagens, was collected every 2 days and EDTA was replenished. Collected EDTA extracts were exhaustively dialysed against double distilled water (ddH₂O) to remove EDTA, and hDDM was recovered by lyophilisation.

To prepare hDDM solution for scaffold physisorption, lyophilised hDDM was re-dissolved to 1 mg/mL in ddH₂O and filtered (0.20 µm) (Sarstedt, Germany) before being aliquot. Protein concentration was measured using a bicinchoninic acid assay (BCA) assay kit (Pierce® BCA Protein assay kit; Thermo Scientific, Rockford, USA).

Physisorption of DDM on scaffolds

Poly(LLA-co-CL) scaffolds were placed in sterile 48-well plates, and 300 µL of 10- or 20-µg/mL hDDM solution was added to cover the scaffold. This was followed by shaking for 30 min at 300 rpm at room temperature (RT) in a plate shaker (MixMate® Eppendorf, Germany) before use.

In vitro hDDM release kinetics

Physisorbed scaffolds were immersed in 500 µL of ddH₂O in glass tubes (Duran®, Wertheim, Germany) and incubated at 37°C in a shaking water bath (Julabo®, SW22, Germany). All the supernatants were collected and replaced with fresh 500 µL ddH₂O at pre-determined time points: 24 h, 4 days, 7 days, 14 days and 21 days. The experiment was performed in triplicates.

Sample preparation for label-free mass spectrometry. Label-free mass spectrometry (MS)-based protein quantification technologies were used in order to estimate relative abundance of protein released from the scaffolds. The supernatant was collected at the pre-determined time points, lyophilised and mixed with urea solution (8 M urea/20 mM methylamine in dH₂O) for de-folding of the protein structure. Then, buffer (50 mM tris/L mM CaCl₂ in dH₂O) was added in order to reduce urea concentration to 1 M, and samples were incubated with shaking at RT for 5 min. For reduction of disulphide bond between cysteine residues, samples were incubated with 100 mM dithiothreitol (DTT) for 1 h at RT. To block cysteine by carbamidomethylation, 200 mM iodoacetamide was added and incubated for 1 h in darkness at RT, following which 100 mM DTT was added to avoid unwanted protease alkylation and was incubated for 10 min at RT. Trypsin was added to digest the protein in a ratio 1/50

(w/w), and the samples were incubated with shaking overnight at 37°C. Formic acid in a final concentration of 1% was used to stop the trypsin action. Samples were purified using Oasis column HLB µElution plate 30 µM (Waters, Milford, MA, USA). Oasis C18 column was activated using the following steps: 80% acetonitrile, 0.1% formic acid was added and centrifuged at 200 g for 1 min. Following activation, columns were washed with 0.1% formic acid and centrifuged. In the next step, tryptic peptides were added to Oasis column and were left in acidic condition. Columns were washed with 0.1% formic acid twice, and the peptides eluted with 70% acetonitrile, 0.1% formic acid. Eluate obtained was lyophilised and suspended in 8 µL of 2% acetonitrile and 0.1% formic acid. The experiment was carried out in triplicates, and the sample preparation and analysis were carried out in one batch.

MS. Trypsinsed sample was loaded onto a pre-column (Dionex, Acclaim PepMap Nano Trap column, C18, 75 µm i.d. × 2 cm, 3 µm) followed by separation on the analytical column (Dionex, Acclaim PepMap100 RSLCnano column, 75 µm × 15 cm, C18, 2 µm) using a Dionex Ultimate NCS-3500RS Liquid chromatography (LC) system (Sunnyvale, CA) coupled online to an Orbitrap Elite Thermo Scientific mass spectrometer. A 60-min LC method using a gradient composition of mobile phase A (0.1% formic acid/2% acetonitrile) and mobile phase B (0.1% formic acid/90% acetonitrile) was used. The gradient increased from 8% to 40% phase B over 30.5 min, then 40%–90% B over 3 min and 90% phase B for 5 min. The peptides were continuously eluted into the Orbitrap mass spectrometer with a flow rate of 280 nL/min. Data dependent acquisition was used in collision-induced dissociation mode, where the mass spectrometer continuously sequenced the seven ions with highest intensity.

Analysis of MS data, protein identification and quantification. MS/MS spectra were searched against a human database using carbamidomethylation of cysteine as a fixed modification and oxidation of methionine and acetyl of the N-terminus as variable modifications. Fragment ion mass tolerance was 0.60 Da, and the parent ion tolerance was 10.0 ppm. Raw files were analysed using Proteome Discoverer (version 2.1.0.81) and Scaffold (version 4.7.5) in order to obtain spectral count for peptides (peptide-spectrum match (PSM)). MS-Amanda, Sequest and X! Tandem were the search engines used. The raw data were also processed with MaxQuant (version 1.5.6.0) and its built-in Andromeda search engine in order to obtain peptide ions' intensity values. Protein identifications were accepted if they could be established at >95% probability to achieve a false discovery rate <1.0% and with high confidence. Proteins that contained similar peptides and could not be differentiated based on MS/MS analysis alone were grouped. Proteins sharing significant peptide evidence were grouped into clusters.

Two softwares, Proteome Discoverer/Scaffold and MaxQuant, were used for data analysis of the raw files. Scaffold analysis was based on spectral counts (PSM) and MaxQuant on intensity of peptide ions present in the sample.

Protein–protein interactions were analysed using the Search Tool for the Retrieval of Interacting Genes/Proteins (STRING) database.²⁵

Nitrogen quantification by high temperature combustion

The relative nitrogen content, which indicates the degree of functionalisation in the scaffolds, was determined by high temperature combustion using a nitrogen analyser (ANTEK 7000; Antek Instruments, TX, USA). Each sample (c.a. 15 mg) was burnt at 1050°C in an oxygen-poor atmosphere where nitrogen is oxidised to NO before being further oxidised to excited NO₂ in ozone. The light emitted, when the excited NO₂ is converted to its standard state, is detected by a photomultiplier tube. Values are reported as nitrogen counts per mg of sample (N counts/mg).

Culture and maintenance of hBMSCs

hBMSCs were expanded in basal culture media of Dulbecco's Modified Eagle Medium (DMEM) (Gibco® life technologies™, UK), supplemented with 10% foetal bovine serum (FBS) and 1% penicillin/streptomycin (Hyclone GE healthcare, UK), and cultured at 37°C in humidified atmosphere supplied with 5% CO₂. The morphology of hBMSCs was regularly observed microscopically (Nikon TS100, Tokyo, Japan) and cells used at passage 5. The hBMSCs were characterised using flow cytometry, which showed that >90% of cells expressed CD73, CD90 and CD105 and lacked expression of CD34 and CD45. Three different experimental groups were set up: (1) hBMSCs were seeded on the poly(LLA-co-CL) scaffolds and cultured in osteogenic medium (hBMSCs basal medium plus 50 µg/mL ascorbic acid, 3.5 mM β-glycerophosphate and 10⁻⁸ M dexamethasone) as the positive control group (abbreviated as OM), (2) poly(LLA-co-CL) scaffolds were physisorbed with 20 µg/mL hDDM before seeding with hBMSCs and cultured in osteogenic medium (abbreviated as DDMOM) and (3) poly(LLA-co-CL) scaffolds were physisorbed with 20 µg/mL hDDM before seeding with hBMSCs and cultured in hBMSCs basal culture medium (abbreviated as DDM).

The hBMSCs were seeded in a seeding density of 1 × 10⁵ per scaffold for cell attachment and proliferation analysis and 2 × 10⁵ per scaffold for gene and protein analysis. Plates were then shaken (MixMate® Eppendorf, Hamburg, Germany) for 1 min to allow even distribution of cells throughout the scaffolds. Cell/scaffold constructs were cultured at 37°C with 5% of CO₂ for 24 h in basal hBMSCs culture medium to ensure the attachment of cells, and the following day, the medium was replaced with the

respective group media. Medium was replaced every third day. The experiments were repeated twice with a minimum of four replicates in each experiment. Data are presented as the average of repeated experiments.

Scanning electron microscope

Adhesion and spreading of hBMSCs seeded on different scaffolds were visualised on days 1 and 3. Scaffolds were fixed with 3% glutaraldehyde for 30 min, dehydrated with different concentrations of ethanol before critical point drying using CO₂ followed by gold palladium sputter coating and examined with a scanning electron microscope (Joel JSM 7400F, Tokyo, Japan) at a voltage of 10 kV.

Metabolic activity of hBMSCs on the different scaffolds

Colorimetric WST-1 assay (WST Roche Diagnostic GmbH, Mannheim, Germany) was used to evaluate viable cell counts of hBMSCs after 24 h, 3 days and 7 days. Briefly, the medium from the cell/scaffold constructs was replaced with WST-1 at the ratio of 1:10 with the respective medium used. Samples were incubated in the dark for 4 h at 37°C in 5% CO₂. A micro-plate reader (BMG LABTECH, GmbH, Germany) at 450 nm was used to measure the absorbance.

Phosphorylated ERK 1/2 levels from seeded hBMSCs

Phosphorylated levels of ERK1/2 that regulate cell proliferation and growth were quantified. The intracellular protein was extracted from the cell/scaffold constructs at 7 and 21 days by incubating the cell/scaffold constructs under shaking conditions at 4°C for 20 min with radioimmunoprecipitation assay (RIPA) buffer (Thermo Scientific), 1 × Halt™ protease inhibitor cocktail and 1 × Halt™ phosphatase inhibitor cocktail (Thermo Scientific, MA, US). This was followed by sonication for 5 min on ice and centrifugation at 16,000g at 4°C for 20 min. The collected supernatant was measured using BCA assay (Pierce® BCA Protein assay kit, Thermo Scientific), following manufacturer's instruction. Phosphorylated and pan intracellular ERK1/2 was measured using ERK1/2 ELISA kit (Sigma-Aldrich Co. LLC, Louis, USA), and the absorbance was measured at 450 nm.

Gene analysis

Total RNA was isolated from cell/scaffold constructs using the RNA isolation kit (Maxwell®, Promega Corporation, Madison, WI, USA) after 7 and 21 days of culture. Nanodrop spectrophotometer (Thermo Scientific) was used to quantify extracted RNA, and cDNA was synthesised using high-capacity complimentary DNA reverse transcription kit (Applied Biosystem®, Foster, CA, USA) following manufacturer's instructions. Real-time quantitative polymerase

chain reaction (RT-PCR) was done on StepOne™ plus RT-PCR system, using TaqMan® gene expression assays (Applied Biosystems®, Carlsbad, CA, USA) for glyceraldehyde-3-phosphate dehydrogenase (GAPDH), inflammatory cytokines (interleukins IL-6 and IL-8), collagen type 1 alpha 2 (Col 1 α 2), osteopontin (SPP1), bone morphogenetic protein-2 (BMP-2), runt-related transcription factor 2 (RUNX2) and alkaline phosphatase (ALP). GAPDH was used as an endogenous control, and comparative Ct method (2- $\Delta\Delta$ Ct) was used to analyse the obtained data.

Protein analysis for extracellular osteogenic expression

Extracellular secretion of Col1 and BMP-2 was quantified using ELISA in the culture medium collected after 7 and 21 days from the cell/scaffold constructs. A sandwich enzyme immunoassay Merta™ CCIP EIA kit for type 1 Collagen (Quidel® Corporation, Markellar Court, USA) was used following manufacturer's instruction, and the absorbance was measured at 405 nm. Extracellular BMP-2 was measured using a Quantikine® ELISA BMP-2 Immunoassay (DBP200, R&D systems® Inc. Minneapolis, USA), following manufacturer's instructions, and the absorbance was measured at 450 nm.

ALP activity

ALP activity in the seeded hBMSCs was measured after 7 and 21 days. Cell/scaffold constructs were sonicated with Triton-X 100 0.1% on ice followed by incubation at -80°C . Following two freeze-thawing cycles at -80°C , samples were incubated with working solution containing Sigma 104® phosphatase substrate (Sigma-Aldrich) and alkaline buffer solution (Sigma-Aldrich). Stop solution (1 M NaOH) was added, and the absorbance measured at 405 nm.

Alizarin red stain

After 21 days, cell/scaffold constructs were washed thrice in phosphate-buffered saline (PBS) and fixed for 30 min in 4% paraformaldehyde (Merck & Co, White House Station, NJ, USA), followed by 2% Alizarin red S powder (Sigma-Aldrich) dissolved in distilled water and pH adjusted to 4.2. Samples were stained for 20 min and imaged with a light microscope. For quantification of Alizarin red stain, 600 μL of 100 μM cetylpyridinium chloride was added into cell/scaffold construct and left to shake overnight. The stain was diluted 1:3 with cetylpyridinium chloride, and the absorbance measured at 540 nm.

Statistical analysis

Data presented were analysed using IBM SPSS statistics 21.0. The results were presented as \pm standard error of mean (SEM) and analysed using one-way analysis of

variance (ANOVA), followed by Tukey's test for multiple comparison. Difference was considered statistically significant when $p < 0.05$.

Results

Protein identification and release kinetics of hDDM from copolymer scaffolds

Total number of identified proteins (excluding keratins) in MaxQuant was 356 and in Scaffold software was 210. Common proteins for both software were 176. Therefore, a total of 390 different proteins were identified.

The proteins were further analysed with the abovementioned criteria (section 'Analysis of MS data, protein identification and quantification'), and proteins with high confidence (390 proteins) were selected and arranged in groups on the basis of biological function and cellular location, as shown in Figure 1. A detailed presentation, including the definition of each protein identified by MaxQuant and/or Scaffold, is added in the Supplementary Section (Table S1).

To better understand the release pattern of the proteins from the physisorbed scaffolds, prothrombin, an abundant protein in the dentine preparation, was selected, and separate graphs were plotted for each concentration (10 or 20 $\mu\text{g}/\text{mL}$) and the relative abundance of proteins from both softwares (spectral count from Scaffold and intensity from MaxQuant software). This was done to compare the robustness and reliability of the two softwares and to compare the release patterns from the different hDDM concentrations (Figure 2). The pattern of release of prothrombin with time was comparable when analysed by both softwares, and the spectral counts and intensity values obtained were higher in the higher concentrations of hDDM (20 $\mu\text{g}/\text{mL}$) compared to the lower. Similarly, a comparable release trend was observed for most proteins from both hDDM concentrations physisorbed scaffolds. Therefore, focus was on data from scaffolds physisorbed with 20 $\mu\text{g}/\text{mL}$ hDDM. Data obtained from the MaxQuant software are illustrated to include maximum number of proteins, considering its higher sensitivity as being previously reported.²⁶

Release pattern and interactions of proteins involved in bone regeneration

Of the 390 released proteins identified by MaxQuant and Scaffold softwares, those proteins essential for bone regeneration were selected for further analysis and included in one of the two categories: growth and maintenance, and signal transduction (Table S1). Proteins from these two categories were analysed for their interactions using STRING software, and proteins with connected networks and with a minimum required interaction score with confidence of 0.700 or higher are shown in Figure 3. In total, number of connected nodes was 111 (out of a total of 126

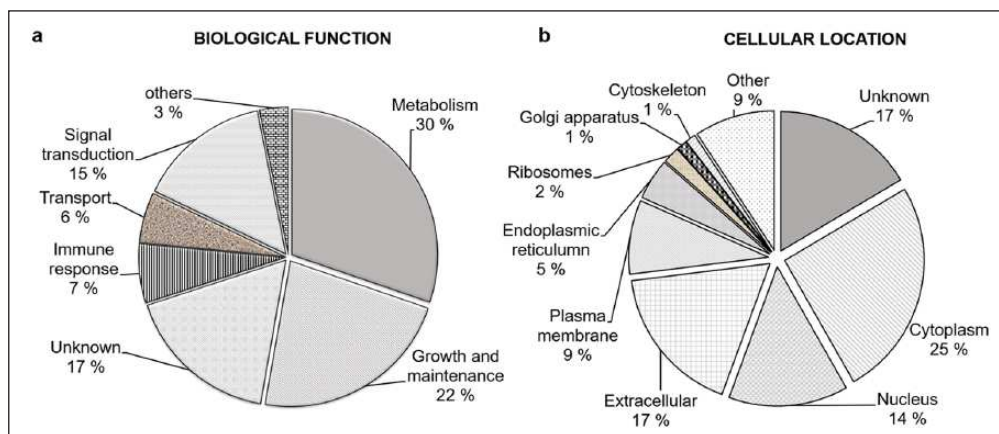


Figure 1. Categorising of hDDM proteins released identified in MaxQuant and Scaffold software: (a) biological function and (b) cellular location.

The protein identification was carried out using the database reference (<http://www.hprd.org/>).

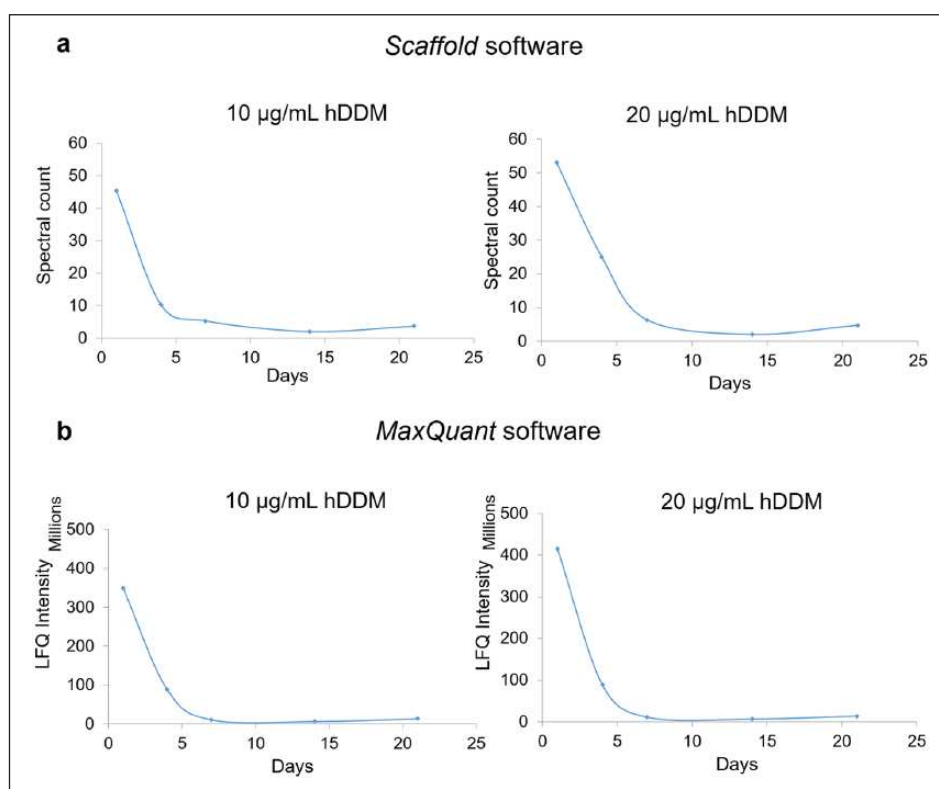


Figure 2. Release pattern of prothrombin from poly(LLA-co-CL) scaffolds physisorbed with 10- or 20- $\mu\text{g}/\text{mL}$ DDM: (a) spectral counts from Scaffold software and (b) intensity values from MaxQuant software.

proteins from both categories) with 123 edges. Therefore, proteins show their effects by interacting with each other. The proteins that showed clear pattern of release and play vital roles in osteogenesis^{10,27} are reported in Table 1 and are carried further for analysis.

Selected proteins showed a comparable pattern of release from the poly(LLA-co-CL) scaffolds physisorbed with 20 $\mu\text{g}/\text{mL}$ hDDM but with a difference

in intensities. An initial burst of release was shown in 24 h from the non-collagenous proteins (biglycan, osteomodulin and osteopontin) (Figure 4a–c); signal transducing protein (TGF- β 1) (Figure 4d); collagen-forming proteins (Coll α 1 and Coll α 2) (Figure 4e and 4f); and the calcium binding proteins (S100A9 and S100A8) (Figure 4g and 4h). The amounts of protein released significantly decreased for all proteins, and a

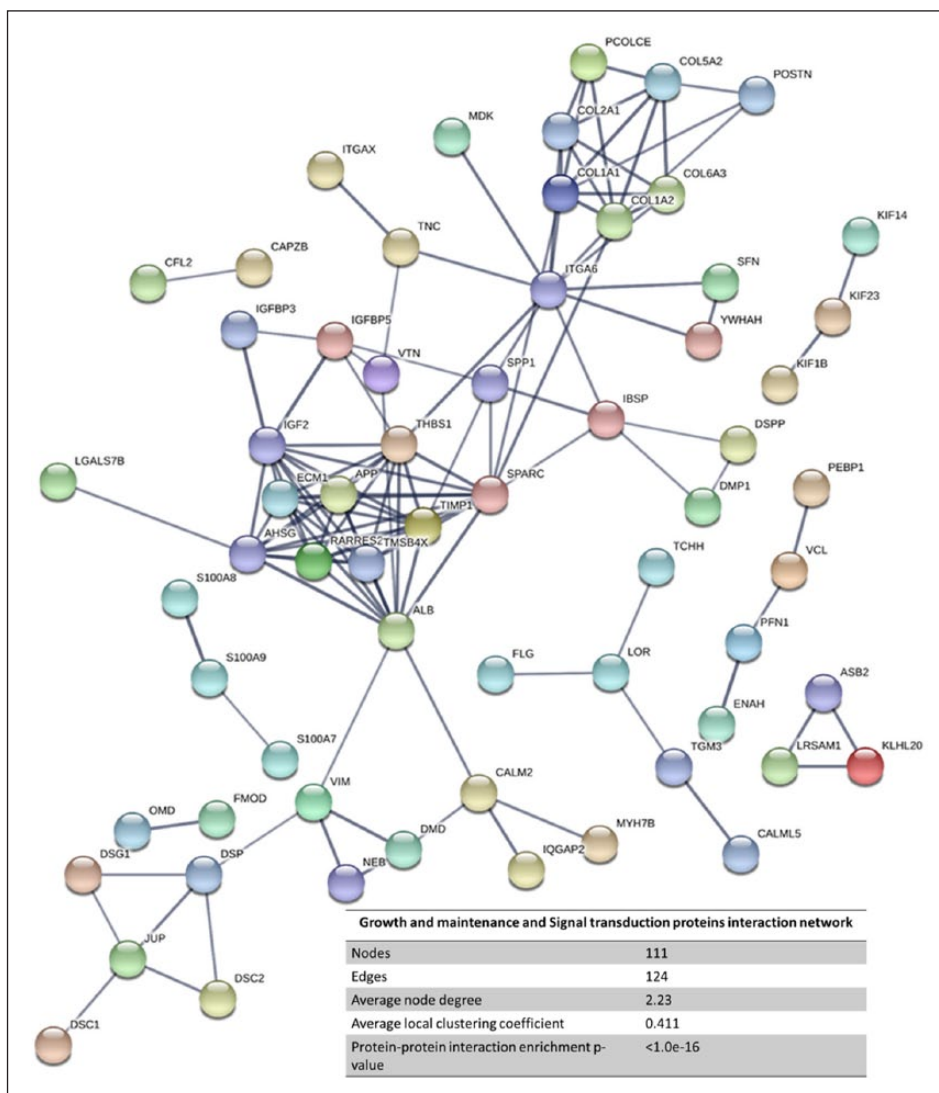


Figure 3. Protein–protein interaction network.

Proteins from growth and maintenance and signal transduction categories visualised by STRING, and the colour saturation of the edges represents the confidence score of a functional association. The nodes indicate proteins, and edges indicate the number of interactions. The number of average interactions per node is indicated by the node degree. The clustering coefficient specifies the average node density of the map. Disconnected nodes are hidden and only interactions with a high confidence score of 0.700 or more are shown.

Table 1. Selected proteins of interest released from copolymer scaffold and involved in bone regeneration.

Selected proteins of interest involved in bone regeneration

Categories	Gene name	Protein name	Peptide count	Biological function
Bone-forming protein	BGN	Biglycan	13	Growth and maintenance
Bone-forming protein	OMD	Osteomodulin	9	Growth and maintenance
Bone-forming protein	SPP1	Osteopontin	2	Growth and maintenance
Signal transducing	TGF- β 1	Transforming growth factor beta-1	5	Signal transducing
Collagen-forming protein	Col1 α 1	Collagen alpha-1	22	Growth and maintenance
Collagen-forming protein	Col1 α 2	Collagen alpha-2	13	Growth and maintenance
Calcium-bonding protein	SI00A9	SI00 calcium binding protein A9	8	Signal transducing
Calcium-bonding protein	SI00A8	SI00 calcium binding protein A8	5	Signal transducing

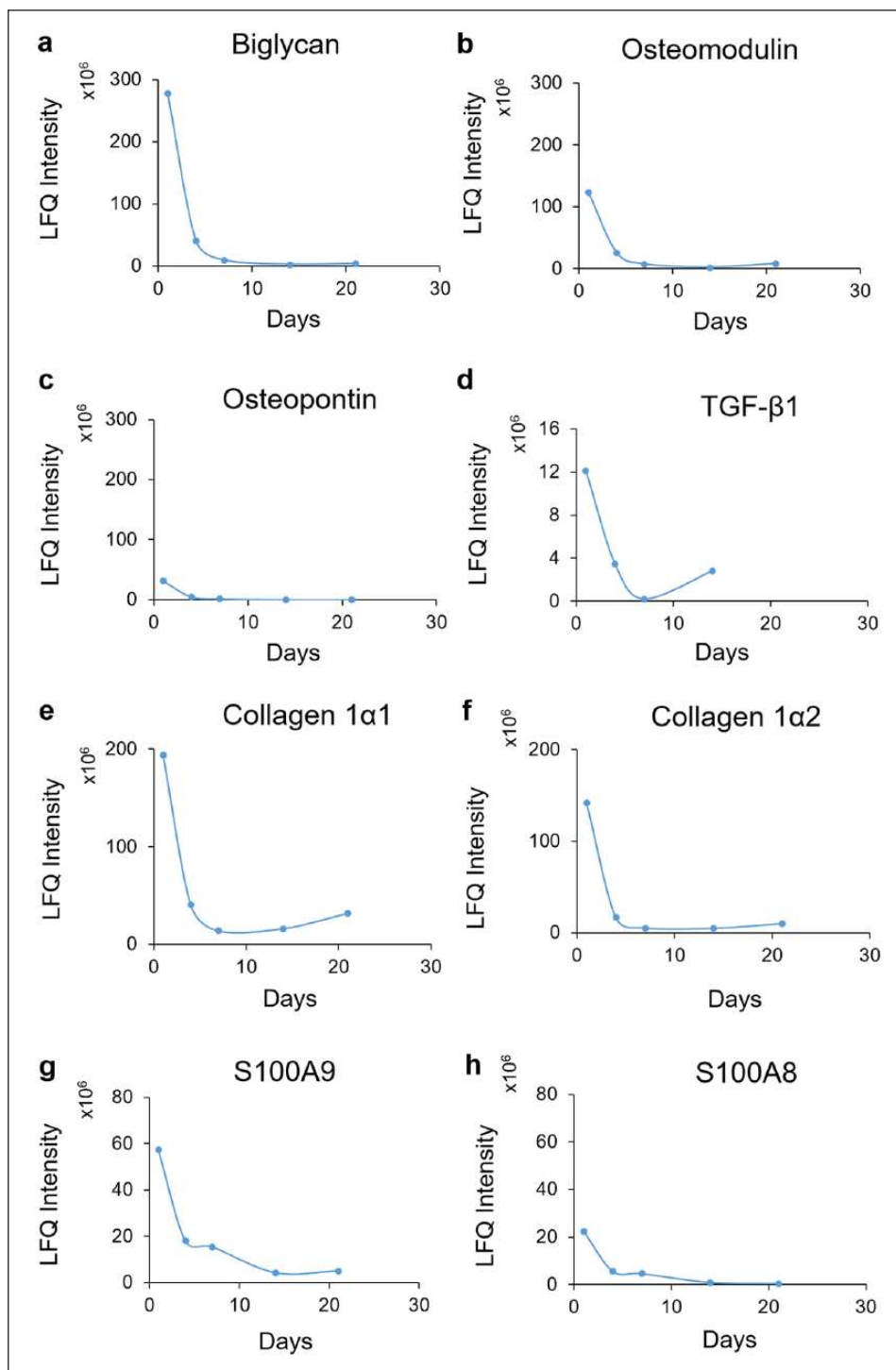


Figure 4. Release pattern of selected proteins involved in bone regeneration: bone-forming proteins: (a) biglycan, (b) osteomodulin and (c) osteopontin; signal transducing protein: (d) transforming growth factor beta I (TGF-β1); collagen-forming proteins: (e) collagen Iα1 and (f) collagen Iα2; calcium binding proteins: (g) S100A9 and (h) S100A8. Data are obtained from MaxQuant software, and y-axis shows intensity of ions that relates to protein abundance and x-axis shows the number of days.

second slight burst of release was found between days 14 and 21 for biglycan, osteomodulin, Coll1α1, Coll1α2, S100A9 and, from day 7 onwards, for TGF-β1, whereas osteopontin and S100A8 showed a continuous decrease in protein release.

Nitrogen quantification from the different scaffolds

To confirm the functionalisation of scaffolds with hDDM and its actual release, nitrogen quantification was carried

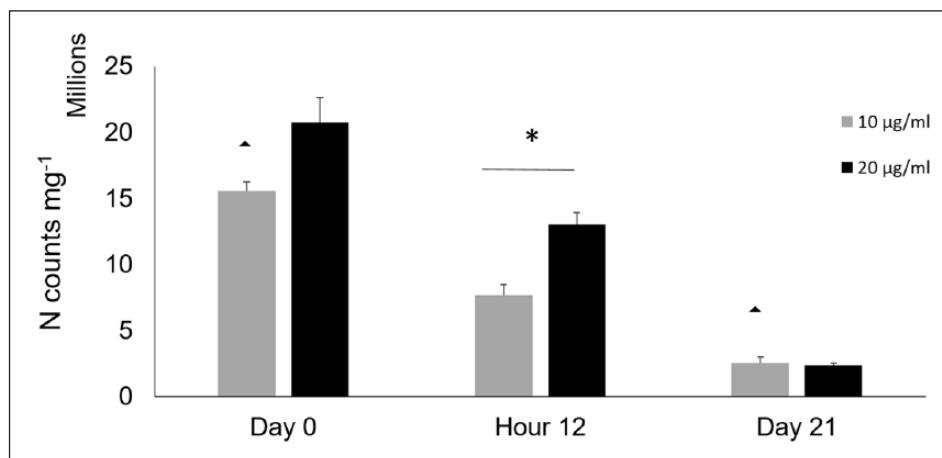


Figure 5. Nitrogen quantification after 0h, 12h and 21 days.

▲ significant with the other time points.

* $p < 0.05$.

out. Results showed that the amount of nitrogen on scaffolds physisorbed with 20µg/mL hDDM was higher than 10-µg/mL hDDM on day 0 and after 12h. The amount of nitrogen on the scaffolds was reduced significantly after 12h and 21 days for both concentrations, indicating the release of proteins from the physisorbed scaffold; however, the amount of protein on scaffolds was almost the same for both concentrations of hDDM at 21 days (Figure 5).

Attachment, viability and proliferation of hBMSCs on the functionalised scaffolds

Scanning electron microscopy of scaffolds after day 1 and day 3 of culture showed hBMSCs attachment, spreading and distribution inside the pores on all scaffold groups (Figure 6a). WST assay showed that the hBMSCs cultured on all scaffold groups continued to proliferate from day 1 to day 7, but to a lesser extent in the DDM group compared to the others groups (Figure 6b). Levels of ERK1/2 phosphorylation were compared with the total ERK (ERK Pan). On days 7 and 21, phosphorylation of ERK1/2 was highest in DDM, although not significant (Figure 6c).

Expression of inflammatory and osteogenic mRNA

Expression of the inflammatory markers IL-6 and IL-8 were significantly higher in DDM group on day 7 compared to the other groups. On day 21, the trend of IL-6 expression was comparable to that at day 7 albeit lower in amount (Figure 7a). After 21 days in DDM, IL-8 revealed a marked decrease in expression compared to the positive control and DDMOM groups (Figure 7a).

The mRNA expression of RUNX2 (Figure 7b) was lower in DDM group compared to OM, but was higher than DDMOM group on days 7 and 21. On day 21, the

RUNX2 expression decreased in OM group, while it increased in the DDM group compared to its expression on day 7. Col1α2 mRNA expression (Figure 7b) was significantly higher on day 7 in DDM group compared to the other groups (OM and DDMOM). Its expression was downregulated on day 21 in all groups, but compared to the other groups on day 21, Col1α2 expression in DDM group was still the highest. ALP mRNA expression by the hBMSCs was significantly lower in the DDM group on day 7 and day 21, compared to the other groups. However, ALP expression was downregulated in OM and DDMOM groups after 21 days, while it continued to upregulate in the DDM group (Figure 7b). The expression of BMP-2 in DDMOM group was comparable to the positive control. The mRNA BMP-2 expression was downregulated in the DDM group after 21 days, but still remained higher than the other groups (Figure 7c). The mRNA expression of osteopontin in experimental group was significantly high when compared to the other groups on both time points. Osteopontin expression was downregulated after 21 days in DDM group; however, it was slightly upregulated in the other groups (Figure 7c).

Extracellular protein secretion

All groups expressed Col1 and BMP-2 protein extracellularly in considerable amounts. The secretion of Col1 was significantly lower in DDM group on day 7, compared to the other groups (Figure 8a). After 21 days, the secretion of Col1 in DDM group increased, compared to a decrease in the other two groups. However, this secretion was not significantly different at day 21 between the groups. As for the secretion of BMP-2, it continued to increase from day 7 to 21 (Figure 8b). At day 7, the highest secretion was in the positive control compared to the highest secretion being in DDM group at 21 days.

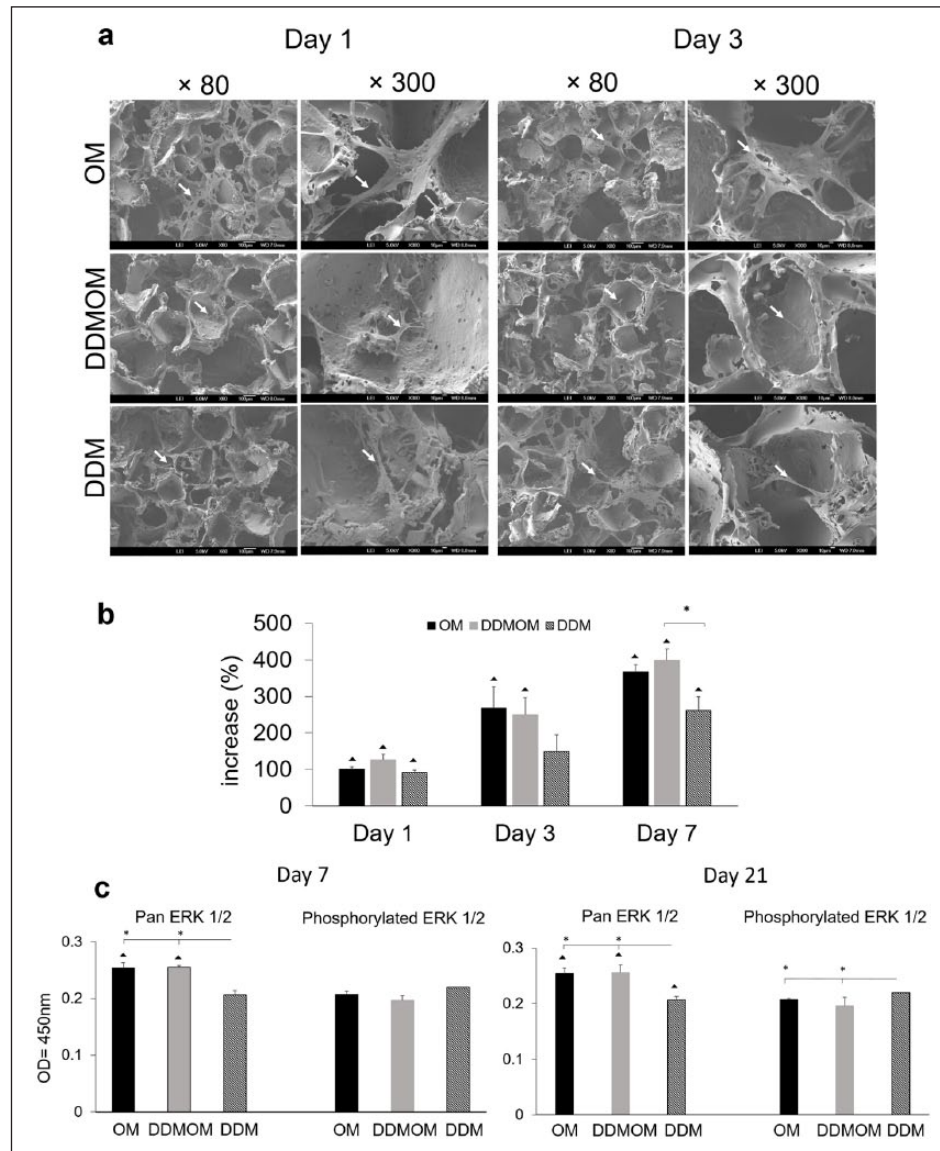


Figure 6. hBMSCs spreading, viability and proliferation. (a) Scanning electron microscope images of hBMSCs spreading on the different scaffolds after 1 and 3 days of culture. The white arrow points to the hBMSCs attached to the scaffolds and distributed through the pores. (b) hBMSCs proliferation in the different scaffold conditions after 1, 3 and 7 days. (c) Levels of ERK1/2 phosphorylation and pan ERK1/2 at 7 and 21 days.

▲ significant difference compared with the other time points.

* $p < 0.05$.

ALP activity and in vitro mineralisation

ALP was significantly lower in the DDM group on day 7, compared to the positive control (OM) and DDMOM group (Figure 9a). Subsequently, the ALP activity significantly increased in the positive control after 21 days, while it reduced slightly in the other two groups containing DDM.

Calcium deposition and mineralisation was assessed by quantification of Alizarin red staining after 21 days of culture and showed successful mineral deposition in all groups. However, mineral deposition in the OM and DDMOM groups was significantly higher compared to the DDM group (Figure 9b).

Discussion

We physisorbed hDDM on poly(LLA-co-CL) scaffolds to render them osteoinductive scaffolds. We studied the protein release kinetics up to 21 days and the efficacy of physisorbed hDDM on the osteogenic differentiation of hBMSCs cultured on these osteoinductive scaffolds after 7 and 21 days.

In this study, in vitro hDDM release was evaluated from copolymer scaffold physisorbed with 10- or 20- $\mu\text{g}/\text{mL}$ concentration of hDDM with LC-MS/MS. It should also be considered that some proteins might not be detected due to ion suppression, a major concern in MS. BMP-2 was not

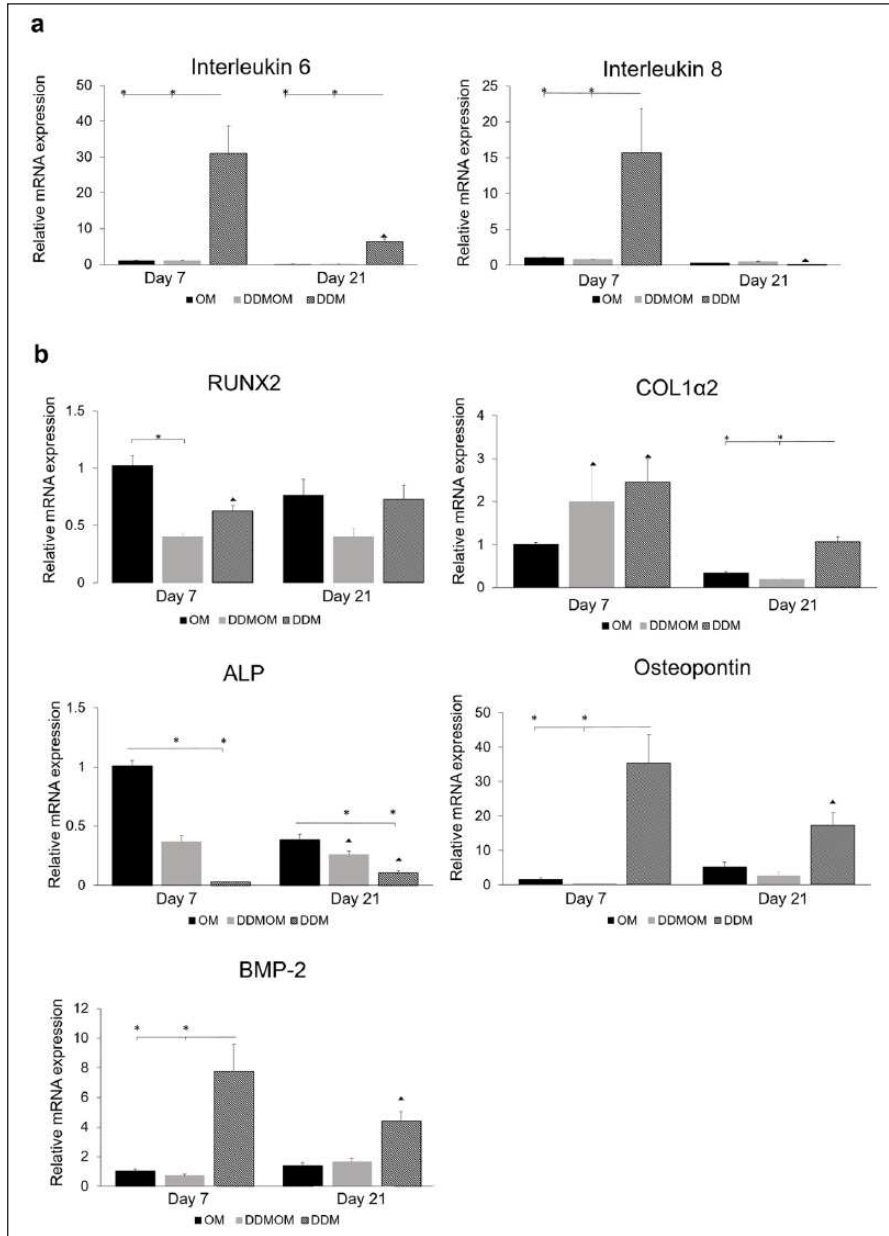


Figure 7. Relative mRNA expressions of inflammatory and osteogenic markers after 7 and 21 days: (a) inflammatory markers IL-6 and IL-8 and (b) early and late osteogenic markers RUNX2, Col1 α 2, osteopontin and ALP.

▲ significant with the other time points.

* $p < 0.05$.

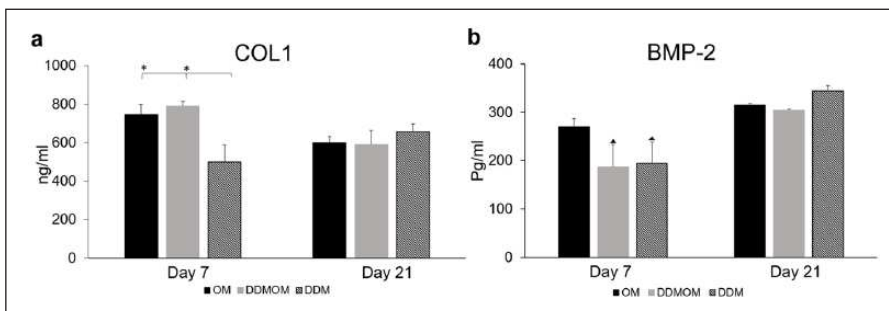


Figure 8. Osteogenic proteins expression extracellularly: (a) COL1 and (b) BMP-2.

▲ significant with the other time points.

* $p < 0.05$.

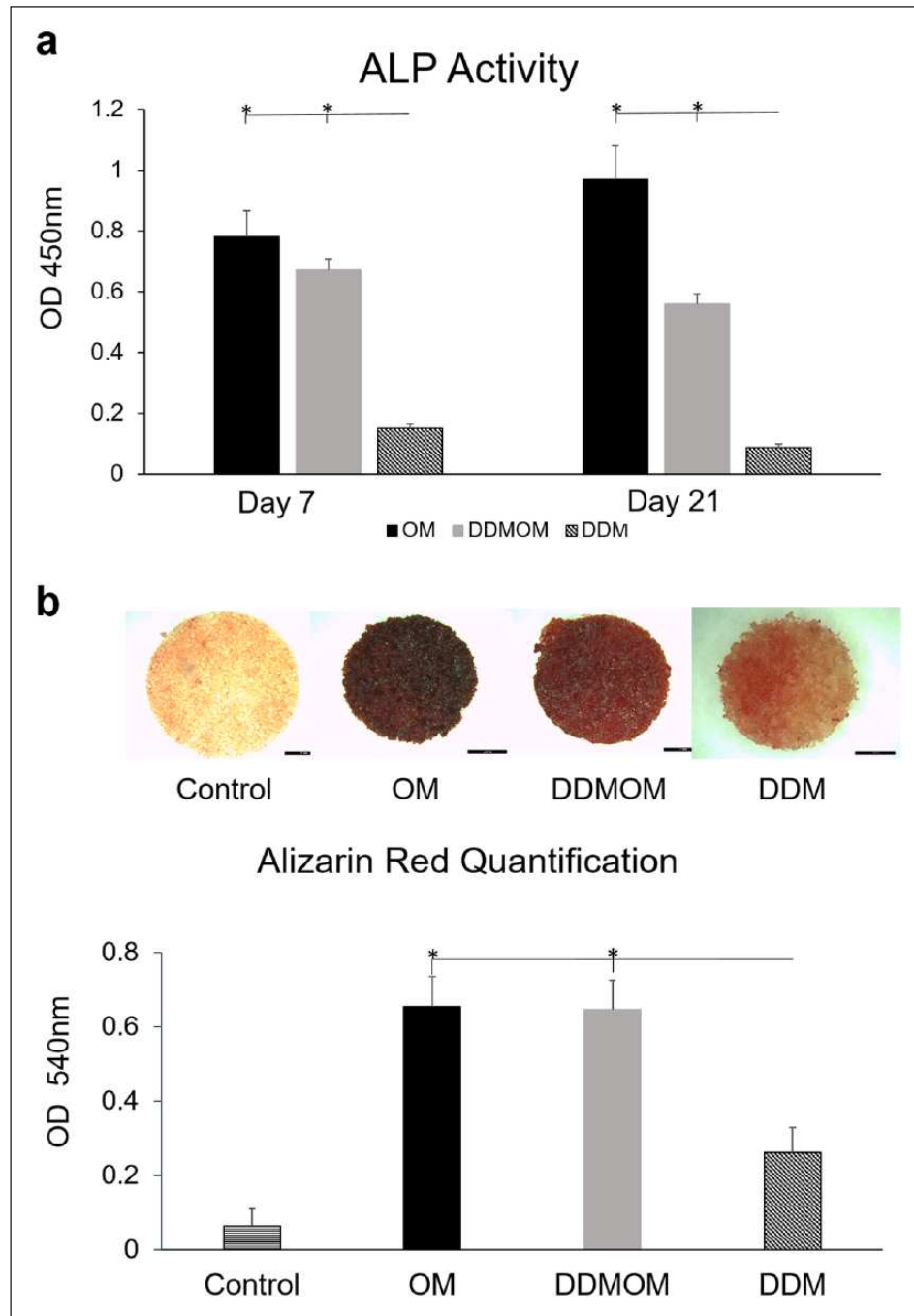


Figure 9. (a) Alkaline phosphatase activity and (b) macrographs of the different scaffolds stained with Alizarin red and quantification of the Alizarin red stain.
* $p < 0.05$.

identified by MS, but was expressed by hBMSCs cultured on the physisorbed scaffolds. A previous study also reported no identification of BMP-2 in their MS analysis of human dentine for similar reasons.⁷ Most of the proteins studied were highly expressed in the first 24 h, indicating their release from the scaffold surface. This rapid release can be explained due to the possible weak bonds of some of the proteins to the scaffold, resulting in a high expression followed by a period of gradual decrease.²⁸ The

nitrogen quantification confirms the physical bonding of the proteins to the scaffold. An early and late release pattern of protein was also reported from BMP-2 on a similar copolymer scaffold, where physisorbed BMP-2 was released in increased amounts after 24 h and a second peak of release was seen after 21 days.¹⁹ However, some proteins in our study showed an exception to the abovementioned release pattern, such as TGF- β . This protein showed a burst release at 24 h and again a peak after 14 days, which

can be hypothesised to the non-covalent protein binding affinity to the copolymer scaffold.²⁹ The conformation of protein structures and surface chemistry of the carrier are all factors that determine how strong the proteins are adsorbed on a surface.³⁰ Poly(LLA-co-CL) scaffolds are hydrophobic,³¹ and the hDDM solution was added to the scaffold without any pre-wetting, which could have affected how the different proteins bound to the scaffolds depending on their structures, thus showing slight differences in the pattern of release between different proteins.

In comparison to previous MS analyses of dentine, where 147–270 proteins were identified,^{8,10} 390 proteins (excluding 11 keratins) were identified in this study. Almost 88% of the proteins from the (growth and maintenance) and (signal transduction) categories in our identified proteins showed interactions, thus highlighting the synergistic functions performed by the growth factors including cell migration and signal transduction for cell proliferation and differentiation into osteoblastic lineage and regulation of bone formation.^{7,9} Interaction of the cells with scaffolds is important for their subsequent cell adhesion, proliferation, maturation and deposition of ECM and its mineralisation. Proliferation of hBMSCs in functionalised and non-functionalised scaffolds demonstrated that the least cell proliferation was in the DDM group. However, a gradual increase in the proliferation from day 1 to 7 was observed in this group. Our results are in line with a previous report that higher concentrations of DDM (10 µg/mL) showed less cellular proliferation and decreased apoptosis compared to lower concentrations of DDM (0.1 µg/mL).⁹ Thus, we can say that high concentrations of hDDM in our study caused less cell proliferation in DDM group and thus initiated the early differentiation. This is also reflected in the upregulated phosphorylated ERK1/2 in DDM group (on both time points) where a presence of cocktail of growth factors released from the functionalised scaffold promotes survival of hBMSCs and osteoblastic differentiation. Phosphorylated ERK1/2 initiates the downregulation pathways in cell and regulates the cell proliferation, differentiation and cell death (apoptosis), and ERK1/2 pathway plays an important role in hBMSCs differentiation into osteogenic lineage.^{32,33} A slightly higher expression of the phosphorylated ERK1/2 at 21 days in the DDM group compared to the pan ERK1/2 expression in the same group could be postulated to be due to a negative regulation effect.

The calcium binding protein S100A9 was highly detected in hDDM released from the functionalised scaffolds. Studies on human gingival fibroblasts have shown that the S100A9 activated the ERK1/2 mitogen-activated protein kinase (MAPK) pathway, as well as promoted the expressions of the inflammatory markers IL-6 and IL-8 in these fibroblasts.³⁴ This supports the trends that were expressed in our experiments, where high levels of S100A9 released coincided with higher phosphorylated ERK1/2 expressions and significantly higher IL-6 and IL-8 expressions in the DDM group. These inflammatory cytokines have important roles in early inflammation and in

osteogenic differentiation for bone regeneration and remodelling.^{35,36} A high expression of pro-inflammatory markers also supports an early initiation of the inflammatory cascade and early differentiation of cells into osteoblastic lineage, followed by a reduction in inflammation at a later time point, such as after 3 weeks in our study. In vivo studies have also reported reduced inflammation with hDDM by reduced white blood cell infiltrate³⁷ and reduced signs of inflammatory infiltrate histologically.³⁸

In vitro osteogenic differentiation potential of the hBMSCs cultured on scaffolds functionalised with hDDM was shown by the expression of early and late osteogenic markers. RUNX2 promotes osteoblast differentiation at an early stage of induction, and it needs to be downregulated after the cell has become a preosteoblast in order to then continue to differentiate into an osteoblast.³⁹ In our study, the expression of RUNX2 in the groups DDM and DDMOM showed an upregulated trend from day 7 to day 21 (although not significant), compared to the downregulated trend in OM from day 7 to day 21. This could indicate a continuation in the transcription in DDM and DDMOM groups; hence, cells are still in the process of differentiating compared to a full differentiation in the cells in OM. Results of our study were similar to another study where BMSCs were cultured with 10 µg/mL DDM concentration and showed high RUNX2 expression when compared to controls and lower hDDM concentrations.⁹ This early differentiation capacity of DDM group is again portrayed with several other early osteogenic markers. The mRNA expression of Col1α2 remained significantly high in DDM group on both time points, but downregulation was noticed on day 21 in all groups. This mRNA expression in DDM group was complemented by a low secretion of Col1 protein on day 7 followed by high protein secretion indicating that early high expression of the gene gives signals to the cells to increase the secretion of collagen-forming proteins. This collagen expression can also be correlated to the release profile of the collagen-forming proteins from the functionalised scaffolds. They were shown to have high expressions that were seen after day 14, especially for Col1α1, and this in turn can influence the relevant expressions in the cultured hBMSCs. ALP and osteopontin have important inverse roles in mineralisation, where ALP partly dephosphorylates osteopontin and acts as an important mineralisation promoter by hydrolysing mineralisation inhibitors.⁴⁰ The ALP mRNA expression was significantly lower in DDM group compared to other groups, but began to increase slightly in DDM after 21 days. However, a study on DPSC showed a different ALP expression, where the ALP level was highest with DDM 1mg/mL concentration and equal in other groups after 5 days, followed by decrease in ALP in both groups supplemented with DDM.⁴¹ This could be related to higher concentrations used in their study that were replaced with every culture medium change as well as the different responses from different cells types. However, in our study, osteopontin was significantly highly expressed in DDM group

compared to other groups, and its expression downregulates and vice versa in other groups. It has been reported that osteopontin regulates mineral deposition in a way that high expression of osteopontin reduces ALP, thus reducing mineralisation.⁴² Accordingly, we can conclude that high early expression of osteopontin resulted in lower expression of ALP, and similarly, as the osteopontin downregulates, ALP expression increases. This can also be related to the high amounts of osteopontin that were detected in the release of hDDM from the scaffolds from the first 24h, which hence influence cultured hBMSCs to start osteopontin production. BMP-2, a member of the TGF- β 1 superfamily, plays an important role in bone formation by stimulating osteoblastic differentiation and augmenting collagen synthesis.⁴³ A significantly higher mRNA expression of BMP-2 was observed in the DDM group after 7 and 21 days. However, after 21 days, BMP-2 mRNA expression was downregulated in DDM group, which is supported by the high BMP-2 protein secretion. High secretion of BMP-2 was also reported in DPSC in which the cells were routinely supplemented with 10mg/mL of DDM concentration.⁴¹ This high BMP-2 expression can be complemented and explained by the high levels of TGF- β 1 released from the functionalised scaffolds initiated from day 7.

A high expression of osteogenic markers from cells cultured in the DDM group and the calcium deposition identified indicate an osteogenic efficacy of the functionalised scaffolds and the early differentiation of hBMSCs into osteoblastic lineage. The OM group received fresh osteogenic molecules with every medium change unlike the DDM group, which could undermine the potential of the DDM group. Also, *in vitro* culture supplement on its own does not cause large volumes of mineralisation, despite an increase in osteogenic genes being expressed by MSCs. This can be due to limited calcium/phosphate availability for which mineral can be synthesised, whereas osteogenic medium contains beta-glycerophosphate as a mineral source to allow extensive mineralisation to occur. In an *in vivo* system, there will naturally be a much higher availability of these so that mineralisation can occur more readily, as has been shown in various studies *in vivo*. Despite the limitations, DDM group still had comparable expressions to OM in the early osteogenic markers, if not higher (e.g. Col1 α 2 and BMP-2). The group DDMOM was expected to have improved osteogenic potential compared to both the DDM and OM group, due to the addition of osteogenic medium delivering potent signals in addition to those already present in hDDM. However, this increase in comparison to DDM was only observed in ALP mRNA and enzyme activity and Col1 at protein level. In comparison to OM, DDMOM showed higher expressions in Col1 at mRNA and protein levels. These inconsistent trends could be due to a synergistic effect of growth factors in demineralised dentine matrix and osteogenic medium that could lead to a negative feedback effect instead of a

positive effect. Previous reports of synergistic effects of two or three growth factors with known concentrations introduced to mesenchymal stem cells culture have shown enhanced osteogenic potential.⁴⁴ However, when a cocktail of growth factors derived from conditioned medium of hBMSCs is combined with osteogenic medium, similar inconsistent patterns of osteogenic markers at mRNA level were observed in human dental pulp cells.⁴⁵ It could also be that in our study, the increase in OM was near maximal in terms of outputs measured and therefore this masked any further increases when hDDM was added. The dynamics of growth factor signalling portrays feedback regulatory components that show different signalling patterns in different types of cells under different stimuli.⁴⁶

Conclusion

Taken together, we conclude that our poly(LLA-co-CL) was in fact bioactive and osteoinductive after being functionalised with hDDM and can facilitate the signals necessary for the osteogenic differentiation of hBMSCs, and hence bone regeneration. Physisorption of hDDM is studied for the first time in our study on poly(LLA-co-CL) scaffolds and showed promising osteogenic potential *in vitro*. This work supports future translation into an *in vivo* model. These scaffolds can also be further functionalised to be able to deliver growth factors from the hDDM and mimic a natural bone regeneration mechanism, that is, delivering/releasing the growth factor in a spatiotemporal manner.

Acknowledgements

The mass spectrometric analysis was carried out at the Proteomics Unit, University of Bergen (PROBE).

Data availability

Data will be made available on request.

Declaration of conflicting interests

The author(s) declared no potential conflicts of interest with respect to the research, authorship and/or publication of this article.

Ethical approval

Isolation of primary hBMSCs was approved by the Regional Committee for Medical and Health Research Ethics in Norway (2013/1248/REK Sør-Øst C).

Funding

The author(s) disclosed receipt of the following financial support for the research, authorship, and/ or publication of this article: The study was funded by Western Norway Regional Health Authority (Helse Vest) (no. 912048) (K.M. and S.S.), Bergen Stem Cell Consortium (no. 502027) (K.M.) and the Swedish Foundation for Strategic Research (A.F.W. and T.F.) (no. RMA15-0010).

ORCID iDsAlastair J Sloan  <https://orcid.org/0000-0002-1791-0903>Salwa Suliman  <https://orcid.org/0000-0003-0385-6157>**Supplemental material**

Supplemental material for this article is available online.

References

- McAllister BS and Haghghat K. Bone augmentation techniques. *J Periodontol* 2007; 78: 377–396.
- Shrivats AR, McDermott MC and Hollinger JO. Bone tissue engineering: state of the union. *Drug Discov Today* 2014; 19(6): 781–786.
- Makhdom AM and Hamdy RC. The role of growth factors on acceleration of bone regeneration during distraction osteogenesis. *Tissue Eng Part B Rev* 2013; 19(5): 442–453.
- Goldberg M, Kulkarni AB, Young M, et al. Dentin: structure, composition and mineralization: the role of dentin ECM in dentin formation and mineralization. *Front Biosci (Elite Ed)* 2011; 3: 711–735.
- Jagr M, Eckhardt A, Pataridis S, et al. Comprehensive proteomic analysis of human dentin. *Eur J Oral Sci* 2012; 120(4): 259–268.
- Gurkan UA, Gargac J and Akkus O. The sequential production profiles of growth factors and their relations to bone volume in ossifying bone marrow explants. *Tissue Eng Part A* 2010; 16(7): 2295–2306.
- Lee CP, Colombo JS, Ayre WN, et al. Elucidating the cellular actions of demineralised dentine matrix extract on a clonal dental pulp stem cell population in orchestrating dental tissue repair. *J Tissue Eng* 2015; 6: 2041731415586318.
- Chun SY, Lee HJ, Choi YA, et al. Analysis of the soluble human tooth proteome and its ability to induce dentin/tooth regeneration. *Tissue Eng Part A* 2010; 17: 181–191.
- Avery S, Sadaghiani L, Sloan A, et al. Analysing the bioactive makeup of demineralised dentine matrix on bone marrow mesenchymal stem cells for enhanced bone repair. *Eur Cell Mater* 2017; 34: 1–14.
- Park E-S, Cho H-S, Kwon T-G, et al. Proteomics analysis of human dentin reveals distinct protein expression profiles. *J Proteome Res* 2009; 8(3): 1338–1346.
- Baker SM, Sugars RV, Wendel M, et al. TGF-beta/extracellular matrix interactions in dentin matrix: a role in regulating sequestration and protection of bioactivity. *Calcif Tissue Int* 2009; 85(1): 66–74.
- Koga T, Minamizato T, Kawai Y, et al. Bone regeneration using dentin matrix depends on the degree of demineralization and particle size. *PLoS ONE* 2016; 11(1): e0147235.
- Reis-Filho CR, Silva ER, Martins AB, et al. Demineralised human dentine matrix stimulates the expression of VEGF and accelerates the bone repair in tooth sockets of rats. *Arch Oral Biol* 2012; 57(5): 469–476.
- Al-Asfour A, Farzad P, Al-Musawi A, et al. Demineralized xenogenic dentin and autogenous bone as onlay grafts to rabbit tibia. *Implant Dent* 2017; 26(2): 232–237.
- Rijal G and Shin H-I. Human tooth-derived biomaterial as a graft substitute for hard tissue regeneration. *Regen Med* 2017; 12(3): 263–273.
- Kabir M, Murata M, Kusano K, et al. Autogenous demineralized dentin graft for third molar socket regeneration a case report. *Dentistry* 2015; 5: 353.
- Kim Y-K, Lee J-H, Um I-W, et al. Guided bone regeneration using demineralized dentin matrix: long-term follow-up. *J Oral Maxillofac Surg* 2016; 74(3): 515e1–515e9.
- Kim Y-K, Kim S-G, Um I-W, et al. Bone grafts using autogenous tooth blocks: a case series. *Implant Dent* 2013; 22(6): 584–589.
- Suliman S, Xing Z, Wu X, et al. Release and bioactivity of bone morphogenetic protein-2 are affected by scaffold binding techniques in vitro and in vivo. *J Control Release* 2015; 197: 148–157.
- Tayalia P and Mooney DJ. Controlled growth factor delivery for tissue engineering. *Advanced Materials* 2009; 21: 3269–3285.
- Melling GE, Colombo JS, Avery SJ, et al. Liposomal delivery of demineralized dentin matrix for dental tissue regeneration. *Tissue Eng Part A* 2018; 24: 1057–1065.
- Idris SB, Arvidson K, Plikk P, et al. Polyester copolymer scaffolds enhance expression of bone markers in osteoblast-like cells. *J Biomed Mater Res A* 2010; 94(2): 631–639.
- Skodje A, Idris SBM, Sun Y, et al. Biodegradable polymer scaffolds loaded with low-dose BMP-2 stimulate periodontal ligament cell differentiation. *J Biomed Mater Res A* 2015; 103(6): 1991–1998.
- Dänmark S, Finne-Wistrand A, Wendel M, et al. Osteogenic differentiation by rat bone marrow stromal cells on customized biodegradable polymer scaffolds. *Journal of Bioactive and Compatible Polymers* 2010; 25: 207–223.
- Szklarczyk D, Franceschini A, Wyder S, et al. STRING v10: protein–protein interaction networks, integrated over the tree of life. *Nucleic Acids Research* 2014; 43: D447–D452.
- Milac TI, Randolph TW and Wang P. Analyzing LC-MS/MS data by spectral count and ion abundance: two case studies. *Stat Interface* 2012; 5(1): 75–87.
- Graneli C, Thorfve A, Ruetschi U, et al. Novel markers of osteogenic and adipogenic differentiation of human bone marrow stromal cells identified using a quantitative proteomics approach. *Stem Cell Res* 2014; 12(1): 153–165.
- Ziegler J, Mayr-Wohlfart U, Kessler S, et al. Adsorption and release properties of growth factors from biodegradable implants. *J Biomed Mater Res* 2002; 59(3): 422–428.
- King WJ and Krebsbach PH. Growth factor delivery: how surface interactions modulate release in vitro and in vivo. *Adv Drug Deliv Rev* 2012; 64(12): 1239–1256.
- Quinlan E, Thompson EM, Matsiko A, et al. Long-term controlled delivery of rhBMP-2 from collagen–hydroxyapatite scaffolds for superior bone tissue regeneration. *J Control Release* 2015; 207: 112–119.
- Sun Y, Finne-Wistrand A, Waag T, et al. Reinforced degradable biocomposite by homogeneously distributed functionalized nanodiamond particles. *Macromol Mater Eng* 2015; 300: 436–447.
- Jaiswal RK, Jaiswal N, Bruder SP, et al. Adult human mesenchymal stem cell differentiation to the osteogenic or adipogenic lineage is regulated by mitogen-activated protein kinase. *J Biol Chem* 2000; 275(13): 9645–9652.
- Mebratu Y and Tesfaigzi Y. How ERK1/2 activation controls cell proliferation and cell death: is subcellular localization the answer. *Cell Cycle* 2009; 8(8): 1168–1175.

34. Gao H, Hou J, Meng H, et al. Proinflammatory effects and mechanisms of calprotectin on human gingival fibroblasts. *J Periodontol Res* 2017; 52(6): 975–983.
35. Prystaz K, Kaiser K, Kovtun A, et al. Distinct effects of IL-6 classic and trans-signaling in bone fracture healing. *Am J Pathol* 2018; 188(2): 474–490.
36. Rothe L, Collin-Osdoby P, Chen Y, et al. Human osteoclasts and osteoclast-like cells synthesize and release high basal and inflammatory stimulated levels of the potent chemokine interleukin-8. *Endocrinology* 1998; 139(10): 4353–4363.
37. Bakhshalian N, Hooshmand S, Campbell SC, et al. Biocompatibility and microstructural analysis of osteopromotive property of allogenic demineralized dentin matrix. *Int J Oral Maxillofac Implants* 2013; 28(6): 1655–1662.
38. Kim S-Y, Kim Y-K, Park Y-H, et al. Evaluation of the healing potential of demineralized dentin matrix fixed with recombinant human bone morphogenetic protein-2 in bone grafts. *Materials* 2017; 10(9): 1049.
39. Komori T. Regulation of osteoblast differentiation by transcription factors. *J Cell Biochem* 2006; 99(5): 1233–1239.
40. Linder CH, Ek-Rylander B, Krumpel M, et al. Bone alkaline phosphatase and tartrate-resistant acid phosphatase: potential co-regulators of bone mineralization. *Calcif Tissue Int* 2017; 101(1): 92–101.
41. Liu G, Xu G, Gao Z, et al. Demineralized dentin matrix induces odontoblastic differentiation of dental pulp stem cells. *Cells Tissues Organs* 2016; 201(1): 65–76.
42. Foster B, Ao M, Salmon C, et al. Osteopontin regulates dentin and alveolar bone development and mineralization. *Bone* 2018; 107: 196–207.
43. Wang RN, Green J, Wang Z, et al. Bone Morphogenetic Protein (BMP) signaling in development and human diseases. *Genes Dis* 2014; 1(1): 87–105.
44. Wang L, Huang Y, Pan K, et al. Osteogenic responses to different concentrations/ratios of BMP-2 and bFGF in bone formation. *Ann Biomed Eng* 2010; 38(1): 77–87.
45. Al-Sharabi N, Xue Y, Fujio M, et al. Bone marrow stromal cell paracrine factors direct osteo/odontogenic differentiation of dental pulp cells. *Tissue Eng Part A* 2014; 20(21–22): 3063–3072.
46. Amit I, Citri A, Shay T, et al. A module of negative feedback regulators defines growth factor signaling. *Nat Genet* 2007; 39(4): 503–512.